Search for Chameleon Particles via Photon Regeneration

Aaron S. Chou[1] for the GammeV Collaboration

[1]Center for Cosmology and Particle Physics, New York University, 4 Washington Place, New York, NY 10003.

DOI: http://dx.doi.org/10.3204/DESY-PROC-2008-02/chou_aaron

We report the first results from the GammeV search for chameleon particles, which may be created via photon-photon interactions within a strong magnetic field. The chameleons are assumed to have matter effects sufficiently strong that they reflect from all solid surfaces of the apparatus, thus evading detection in our previous search for weakly-interacting axion-like particles. We implement a novel technique to create and trap the reflective particles within a jar and to detect them later via their afterglow as they slowly convert back into photons. These measurements provide the first experimental constraints on the couplings of chameleons to photons.

1 Chameleons

Cosmological observations over the past decade have demonstrated with increasing significance the existence of a cosmic acceleration, usually attributed to a negative pressure substance known as *dark energy*. The chameleon mechanism, in which field gains an environment-dependent effective mass, has been proposed as a possible explanation of dark energy [1, 2].

Chameleons may also have axion-like couplings to photons such as $\beta_\gamma(\phi/M_{\rm Pl})F^{\mu\nu}F_{\mu\nu}$ or $\beta_\gamma(\phi/M_{\rm Pl})\tilde{F}^{\mu\nu}F_{\mu\nu}$ where β_γ is a dimensionless coupling parameter. Such a coupling allows photons to oscillate into chameleons and back in the presence of an external magnetic field. The couplings of chameleons to matter and the electromagnetic field induce an effective potential

$$V_{\rm eff}(\phi,\vec{x}) = V(\phi) + e^{\beta_{\rm m}\phi/M_{\rm Pl}}\rho_{\rm m}(\vec{x}) + e^{\beta_\gamma\phi/M_{\rm Pl}}\rho_\gamma(\vec{x}), \tag{1}$$

where $\rho_{\rm m}$ is the background matter density and we have defined the effective electromagnetic field density $\rho_\gamma = \frac{1}{2}(|\vec{B}^2| - |\vec{E}|^2)$ (for scalars) or $\rho_\gamma = \vec{E}\cdot\vec{B}$ (for pseudoscalars) rather than the energy density. Thus the effective mass of the chameleon, $m_{\rm eff} \equiv \sqrt{d^2V_{\rm eff}/d\phi^2}$, evaluated at the minimum of the potential, will depend on the background energy density. A chameleon with large coupling $\beta_{\rm m}$ to matter will become massive inside typical laboratory materials. A chameleon may be trapped inside a "jar" if its total energy ω is less than what its effective mass would be within the material of the walls of the jar. In this case, the walls reflect the incoming chameleons. Chameleons produced from photon oscillation in an optically transparent chamber will be confined until they regenerate photons, which emerge as an afterglow once the original photon source is turned off [3, 4, 5]. The GammeV experiment in its second incarnation is designed to search for such an afterglow and to measure or constrain the possible coupling of chameleons to photons.

2 Afterglow from a jar of chameleons

The GammeV apparatus, described in [6, 7], consists of a long stainless steel cylindrical vacuum chamber inserted into the bore of a $B = 5$ T, $L = 6$ m Tevatron dipole magnet. The entrance and exit of the chamber are sealed with BK7 vacuum windows. A 20 Hz pulsed Nd:YAG laser emits $\omega = 2.33$ eV photons into the chamber at a rate of $F_\gamma \sim 10^{19}$ photons/sec. The 1 cm^{-1} laser linewidth is sufficiently large to span the discrete energy levels of the trapped chameleons.

Interactions with the magnetic field cause each photon to oscillate into a superposition of photon and chameleon states. This superposition can be measured in a quantum mechanical sense through collisions with the windows; chameleons bounce, while photons pass through. The probability for producing a chameleon is obtained from the usual photon-axion oscillation formula $\mathcal{P}_{\rm pr} = \frac{4\beta_\gamma^2 B^2 \omega^2}{M_{\rm Pl}^2 m_{\rm eff}^4} \times \sin^2\left(\frac{m_{\rm eff}^2 L}{4\omega}\right)$. In order to populate the jar with chameleons, the laser is operated continuously for $\tau_{\rm pr} \approx 5$ h. After emerging through the exit window of the chamber, the beam is reflected back through the chamber in order to increase the chameleon production rate and facilitate monitoring of the laser power.

During the afterglow phase of the experiment, the laser is turned off and a low-noise photomultiplier tube placed at the exit window is uncovered. Chameleons interacting with the magnetic field oscillate back into photons, some of which escape to be detected by the PMT. Data are taken in two separate runs, with the polarization vector of the laser either aligned with or perpendicular to the magnetic field, to search for pseudoscalar as well as scalar chameleons.

Throughout the production and afterglow phases, a pressure $P_{\rm chamber} \approx 10^{-7}$ Torr is maintained inside the vacuum chamber using a turbomolecular pump connected to a roughing pump. Because the low-mass chameleons are highly relativistic inside the chamber, the turbo pump simply acts as extra volume (0.026 m^3) for the chameleons. The positive displacement roughing pump is however the weakest "wall" of the chamber, and chameleons must be able to reflect ($m_{\rm eff} > \omega$) on the higher pressure $P_{\rm rough} = 1.9 \times 10^{-3}$ Torr residual gas at the intake of the roughing pump. Furthermore, our experiment is only sensitive to models in which the chameleon is sufficiently light for coherent oscillation in the chamber, $m_{\rm eff} \ll m_{\rm osc} = \sqrt{4\pi\omega/L} = 9.8 \times 10^{-4}$ eV at $P = P_{\rm chamber}$. For a variety of chameleon models, the effective chameleon mass scales with ambient density as $m_{\rm eff}(\rho) \propto \rho^\alpha$, for α of order unity. Our limits on the coupling β_γ will only be valid for models in which the predicted density scaling is strong enough to satisfy both the containment condition at higher ambient density and the coherence condition ant lower ambient density. If $m_{\rm eff}$ is dominated by interactions with the residual gas rather than by interactions with the magnetic energy density, then $m_{\rm eff} = m_0(P/P_{\rm rough})^\alpha$, our constraints on β_γ are valid for models with $\alpha \gtrsim 0.8$ and $\omega < m_0 < m_{\rm osc}(P_{\rm rough}/P_{\rm chamber})^\alpha$. Otherwise, the range of sensitivity in α is even more restricted. Since in our apparatus, $\rho_{\rm m} \approx \rho_\gamma \approx 2 \times 10^{-13}$g/cm^3, the experiment is mainly sensitive to models in which $\beta_{\rm m} \gg \beta_\gamma$ which in addition predict large α.

The prediction of the afterglow rate is complicated by the fact that repeated bounces from imperfectly aligned windows and chamber walls cause chameleon momenta to become isotropic. The coupled photon-chameleon equations must then be integrated along all possible trajectories within the chamber. We model a bounce from the chamber wall as a partial measurement in which the regenerated photon amplitude is attenuated by a factor of $f_{\rm ref}^{1/2}$, where $f_{\rm ref}$ is the reflectivity. The mean decay rate $\Gamma_{\rm dec}$ per chameleon is found by averaging over all trajectories and accounting for losses due to escape or absorption of regenerated photons. Although the cylinder walls are not polished, a low absorptivity $1 - f_{\rm ref} = 0.1$ is assumed in order to overpredict

the coherent build-up of photon amplitude over multiple bounces. This overprediction of the decay rate of the signal results in a more conservative limit on the coupling constant. We obtain an afterglow decay rate $\Gamma_{\rm dec} = 9.0 \times 10^{-5}$ Hz for $\beta_\gamma = 10^{12}$, with $\Gamma_{\rm dec} \propto \beta_\gamma^2$.

The signal itself is conservatively underpredicted as follows. While the laser is on, new chameleons are produced at the rate of $F_\gamma \mathcal{P}_{\rm pr}$ and decay at the rate of $N_\phi \Gamma_{\rm dec}$. After a time $\tau_{\rm pr}$ the laser is turned off, and the chamber contains $N_\phi^{(\rm max)} = F_\gamma \mathcal{P}_{\rm pr} \Gamma_{\rm dec}^{-1}(1 - e^{-\Gamma_{\rm dec}\tau_{\rm pr}})$ chameleon particles. For our apparatus, this saturates at 3.6×10^{12} for $\beta_\gamma \gtrsim 10^{12}$ and small $m_{\rm eff}$. The contribution to the afterglow photon rate from non-bouncing chameleon trajectories is

$$F_{\rm aft}(t) = \frac{\epsilon_{\rm det} f_{\rm vol} f_{\rm esc} F_\gamma {\mathcal{P}_{\rm pr}}^2 c}{\ell_{\rm tot} \Gamma_{\rm dec}} \left(1 - e^{-\Gamma_{\rm dec}\tau_{\rm pr}}\right) e^{-\Gamma_{\rm dec} t}, \qquad (2)$$

for $t \geq 0$, where $t = 0$ is the time at which the laser is turned off. The detector efficiency $\epsilon_{\rm det}$ contains the 0.92 optical transport efficiency, as well as the 0.387 quantum efficiency and 0.7 collection efficiency of the PMT. Because chameleons in the turbo pump region do not regenerate photons, we consider only the chameleons in the cylindrical chamber, which represents a volume fraction $f_{\rm vol} = 0.40$ of the total population. A fraction $f_{\rm esc} = 5.3 \times 10^{-7}$ of chameleons travel the entire distance $\ell_{\rm tot}$ from entrance to exit windows without colliding with the chamber walls, and are focussed by a 2" lens onto the photocathode. While many chameleons that bounce from the walls may also produce photons which reach the detector (indeed, most of the photons that can reach the detector are on bouncing trajectories), such collisions result in a model-dependent chameleon-photon phase shift [8] which can affect the coherence of the oscillation on bouncing trajectories. Our goal here is to present results that are independent of the chameleon model and can thus be applied more generally. We therefore consider only the direct light from non-bouncing trajectories in order to predict the minimum possible afterglow rate for any β_γ and $m_{\rm eff}$. Furthermore, we apply the maximum possible decay rate $\Gamma_{\rm dec}$ in Eq. 2 to allow for the possibility that the afterglow could disappear before we can turn on the detector. Figure 1 shows the expected photon afterglow rate for several values of the photon-chameleon coupling β_γ. Non-observation of this underpredicted rate sets the most conservative limits.

3 Results

No significant excess above the PMT dark rate is seen. In order to minimize the effects of systematic uncertainties due to fluctuations in the dark rate, we compare the expected afterglow signal averaged over the entire observation time to the mean signal observed by the PMT. The dominant uncertainty in our measurements of the chameleon afterglow rate is the systematic uncertainty in the PMT dark rate. We estimate this quantity, using data from [6], by averaging the count rate in each of 55 non-overlapping samples approximately one hour in length. The dark rate, computed by averaging the sample means, is 115 Hz, with a standard deviation of 12.0 Hz. This systematic variation in the dark rate is significantly larger than the statistical uncertainty in the individual sample means. Thus our 3σ upper bound on the mean afterglow rate is 36 Hz above the mean of the data rate for each run, after the 115 Hz average dark rate has been subtracted.

For each $m_{\rm eff}$ and β_γ we predict the total number of excess photons expected within the observation time window. Figure 2 shows the regions excluded by GammeV in the $(m_{\rm eff}, \beta_\gamma)$ parameter space for scalar and pseudoscalar chameleon particles. At $m_{\rm eff}$ near $\sqrt{4\pi\omega/L} = 9.8\times$

10^{-4} eV, our exclusion region is limited by destructive interference in chameleon production. At higher $m_{\rm eff}$, a larger β_γ is needed to produce an equivalent non-bouncing minimum signal rate. However, for $\beta_\gamma \gtrsim 10^{13}$ our sensitivity diminishes because, as shown in Fig. 1, the chameleon decay time $\Gamma_{\rm dec}^{-1}$ in GammeV could be less than the few hundred seconds required to switch on the PMT. In summary, GammeV has carried out the first search for chameleon afterglow, a unique signature of photon-coupled chameleons. Figure 2 presents conservative constraints in a model-independent manner, over a restricted range of chameleon models.

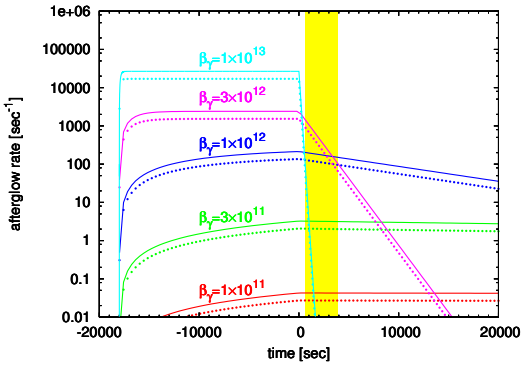

Figure 1: Expected chameleon to photon conversion rate for various values of the coupling to photons β_γ. The solid curves are for chameleons with masses of 10^{-4} eV while the dotted curves are for 5×10^{-4} eV chameleons. Our observation time window for pseudoscalar chameleons is shown shaded in yellow; the corresponding time window for scalar chameleons is shifted to the right by about 700 sec.

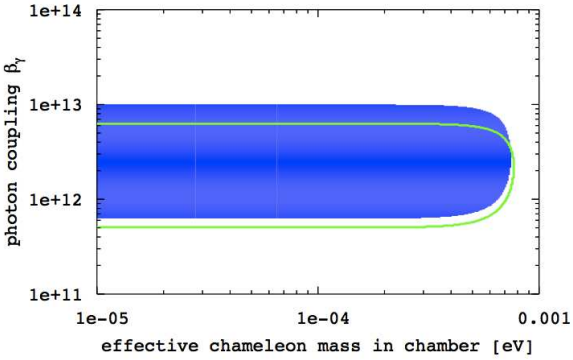

Figure 2: Region excluded by GammeV to 3σ for pseudoscalar (solid blue region) and scalar particles (region between green lines). Constraints worsen at $m_{\rm eff} \gtrsim 10^{-3}$ eV as photon-chameleon oscillation becomes incoherent. These constraints are valid only for models in which the mass scales quickly enough with background density that both the containment and coherence conditions are satisfied.

Acknowledgements: This work is supported by the U.S. Department of Energy under contract No. DE-AC02-07CH11359 and by the U.S. National Science Foundation by NSF-PHY-0401232.

References

[1] J. Khoury and A. Weltman. *Phys. Rev. Lett.*, 93, 2004. 171104.

[2] J. Khoury and A. Weltman. *Phys. Rev. D*, 69, 2004. 044026.

[3] The "particle trapped in a jar" technique was developed as part of the GammeV experiment, and independently realized in [4, 5].

[4] M. Ahlers, A. Lindner, A. Ringwald, L. Schrempp, and C. Weniger. *Phys. Rev. D.*, 77, 2008. 015018 [arXiv:0710.1555 [hep-ph]].

[5] H. Gies, D. F. Mota, and D. J. Shaw. *Phys. Rev. D.*, 77, 2008. 025016 [arXiv:0710.1556 [hep-ph]].

[6] A. S. Chou and others [GammeV (T-969) Collaboration]. *Phys. Rev. Lett.*, 100, 2008. 080402 [arXiv:0710.3783 [hep-ex]].

[7] Aaron S. Chou et al. [arXiv:0806.2438 [hep-ex]].

[8] P. Brax, C. van de Bruck, A. C. Davis, D. F. Mota, and D. J. Shaw. *Phys. Rev. D*, 76, 2007. 085010 [arXiv:0707.2801 [hep-ph]].